On multigrid methods for the Cahn–Hilliard equation with obstacle potential

Ľubomír Baňas

Department of Mathematics
Imperial College London

Joint work with Robert Nürnberg

http://www.ma.ic.ac.uk/~lubo
lubo@imperial.ac.uk

Overview

1. Introduction
2. Continuous model
3. Numerical Method
4. Solvers for the discrete system
5. Numerical experiments

Introduction

Evolution of surfaces applications in material science (microstructure prediction, material proterties, void electromigration in semiconductors), image processing, etc.
Overview Deckekelnick, Dzuik, Elliott (2005)

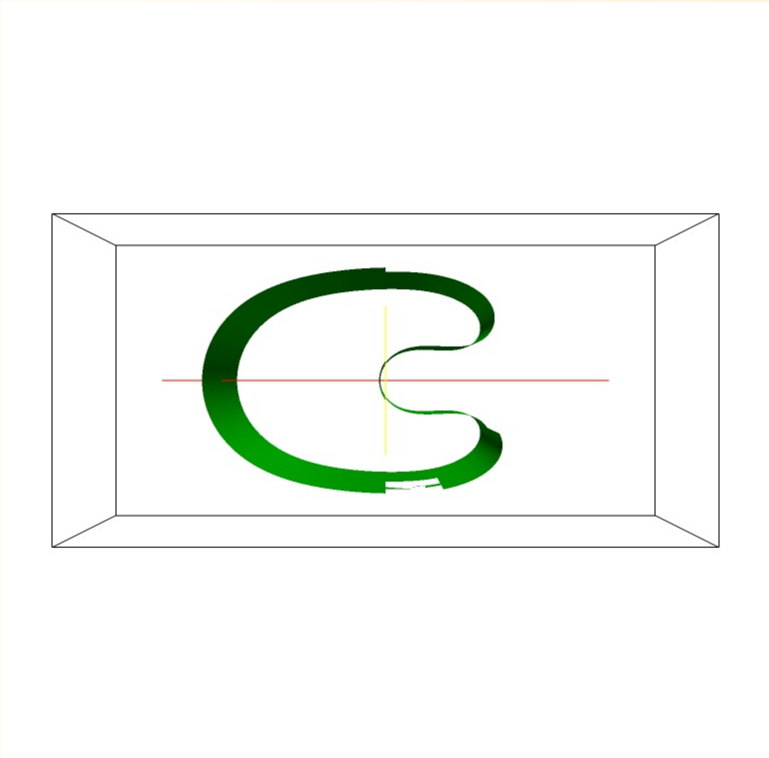

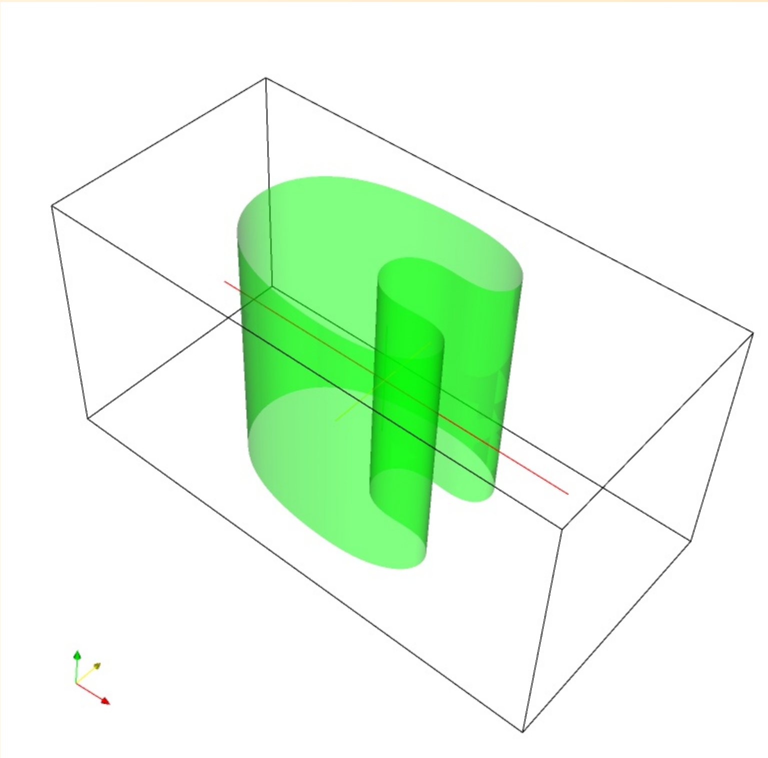

Introduction

Surface diffusion sharp interface model

$$V = -\Delta_s \kappa \qquad \text{on } \Gamma(t)$$

- $\Gamma(t)$ void surface
- Δ_s surface Laplacian
- V velocity of $\Gamma(t)$
- κ curvature

Phase-field model

Diffuse interface with interface width $\approx \gamma\pi$

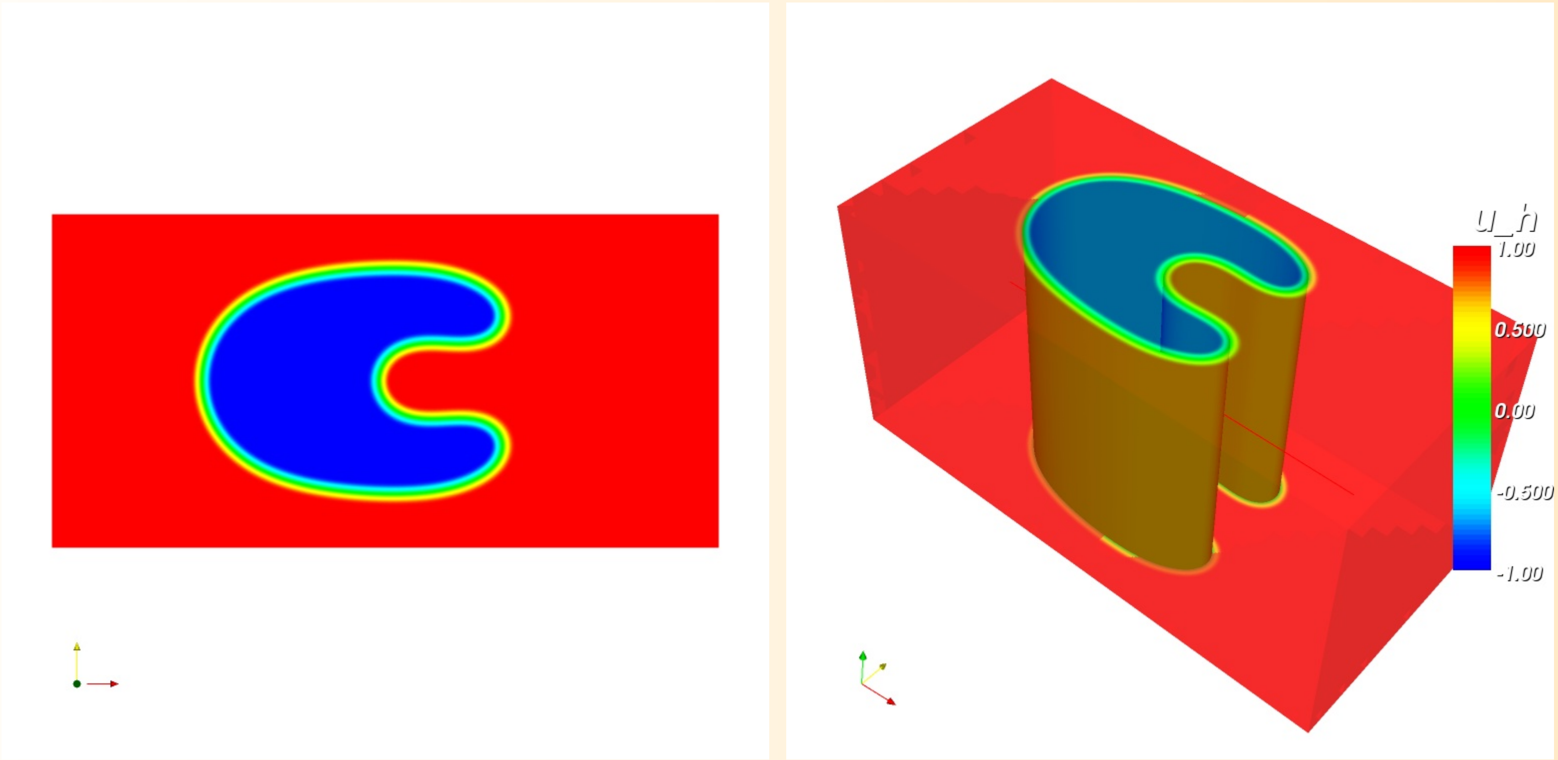

Alternatives to phase-field approach

- Direct methods for approximation of the surface diffusion model, problems with topological changes
- Level set methods can handle topological changes

Phase-field model

- $\gamma > 0$ interfacial parameter
- $u_\gamma(\cdot, t) \in \mathcal{K} := [-1, 1]$, $t \in [0, T]$ conserved order parameter; $u_\gamma(\cdot, t) = -1$ void, $u_\gamma(\cdot, t) = 1$ conductor
- $w_\gamma(\cdot, t)$ chemical potential
- $\phi_\gamma(\cdot, t)$ electric potential

Phase field approximation of surface diffusion (diffuse interface)

$$
\begin{aligned}
&\gamma \frac{\partial u_\gamma}{\partial t} - \nabla.(\, b(u_\gamma)\, \nabla w_\gamma \,) = 0 && \text{in } \Omega_T := \Omega \times (0, T], \\
&w_\gamma = -\gamma\, \Delta u_\gamma + \gamma^{-1}\, \Psi'(u_\gamma) && \text{in } \Omega_T, \text{ where } |u_\gamma| < 1,
\end{aligned}
$$

+ I.C. + B.C.

Phase-field model

Degenerate coefficients

$b(s) := 1 - s^2, \qquad \forall\ s \in \mathcal{K}$

Obstacle-free energy

$$\Psi(s) := \begin{cases} \frac{1}{2}\left(1 - s^2\right) & \text{if} \quad s \in \mathcal{K}, \\ \infty & \text{if} \quad s \notin \mathcal{K}, \end{cases}$$

restricts $u_\gamma(\cdot,\cdot) \in \mathcal{K}$.

Approximation of the sharp interface model $\gamma \to 0$ then $\{x; u_\gamma(x,t) = 0\} \to \Gamma(t)$, $\Gamma(t)$ is the solution of the sharp interface problem

Advantages of phase-field approach

- no explicit tracking of the interface needed
- can handle topological changes

Numerical approximation

$$U_\varepsilon^n \in S^h \Leftrightarrow u_\gamma$$
$$W_\varepsilon^n \in K^h \Leftrightarrow w_\gamma$$
$$\Phi_\varepsilon^n \in S^h \Leftrightarrow \phi_\gamma$$

Double obstacle formulation (ε regularisation parameter)

$$\gamma\left(\frac{U_\varepsilon^n - U_\varepsilon^{n-1}}{\tau_n}, \chi\right)^h + (\Xi_\varepsilon(U_\varepsilon^{n-1})\,\nabla W_\varepsilon^n,\, \nabla\chi) = 0 \qquad \forall\, \chi \in S^h,$$
$$\gamma\,(\nabla U_\varepsilon^n, \nabla[\chi - U_\varepsilon^n]) \geq (W_\varepsilon^n + \gamma^{-1}\, U_\varepsilon^{n-1}, \chi - U_\varepsilon^n)^h \qquad \forall\, \chi \in K^h,$$

discrete inner product (mass lumping) $(\eta_1, \eta_2)^h := \int_\Omega \pi^h(\eta_1(x)\,\eta_2(x))\,\mathrm{d}x$

$$\Xi_\varepsilon(\cdot) \quad \approx \quad b(\cdot)$$

Convergence (Existence) 2D: Barrett, Nürnberg, Styles (2004), 3D: Baňas, Nürnberg (2006) $h \to 0$, $\varepsilon \to 0$, $\tau = \mathcal{O}(h^2)$

Matrix formulation

The discrete system

Find $\{\underline{U}_\varepsilon^n, \underline{W}_\varepsilon^n\} \in \mathcal{K}^{\mathcal{J}} \times \mathbb{R}^{\mathcal{J}}$ such that

$$\begin{aligned}
\gamma\,(\underline{V} - \underline{U}_\varepsilon^n)^T\, B\, \underline{U}_\varepsilon^n - (\underline{V} - \underline{U}_\varepsilon^n)^T\, M\, \underline{W}_\varepsilon^n \quad &\geq \quad (\underline{V} - \underline{U}_\varepsilon^n)^T\, \underline{s} \qquad \forall\, \underline{V} \in \mathcal{K}^{\mathcal{J}}, \\
\gamma\, M\, \underline{U}_\varepsilon^n + \tau_n\, A^{n-1}\, \underline{W}_\varepsilon^n \quad &= \quad \underline{r}
\end{aligned}$$

$$M_{ij} := (\chi_i, \chi_j)^h, \qquad B_{ij} := (\nabla\chi_i, \nabla\chi_j), \qquad A_{ij}^{n-1} := (\Xi_\varepsilon(U_\varepsilon^{n-1})\, \nabla\chi_i, \nabla\chi_j)$$
$$\underline{r} := \gamma\, M\, \underline{U}_\varepsilon^{n-1} - \alpha\, \tau_n\, A^{n-1}\, \underline{\Phi}_\varepsilon^n \in \mathbb{R}^{\mathcal{J}}, \qquad \underline{s} := \gamma^{-1}\, M\, \underline{U}_\varepsilon^{n-1} \in \mathbb{R}^{\mathcal{J}}.$$

Block Gauss-Seidel algorithm with projection

Projected block Gauss-Seidel

$$\begin{aligned}(\underline{V} - \underline{U}_\varepsilon^{n,k})^T (\gamma\,(B_D - B_L)\,\underline{U}_\varepsilon^{n,k} - M\,\underline{W}_\varepsilon^{n,k}) &\geq (\underline{V} - \underline{U}_\varepsilon^{n,k})^T (\underline{s} + \gamma\, B_L^T\,\underline{U}_\varepsilon^{n,k-1}) \\ \gamma\, M\,\underline{U}_\varepsilon^{n,k} + \tau_n\,(A_D - A_L)\,\underline{W}_\varepsilon^{n,k} &= \underline{r} + \tau_n\, A_L^T\,\underline{W}_\varepsilon^{n,k-1}\end{aligned}$$

2×2 system for every vertex; explicit solution

$$\left[\underline{U}_\varepsilon^{n,k}\right]_j = \left[\frac{M_{jj}\,\widehat{\underline{r}}_j + \tau_n\, A_{jj}^{n-1}\,\widehat{\underline{s}}_j}{\gamma\,[M_{jj}]^2 + \tau_n\,\gamma\, A_{jj}^{n-1}\, B_{jj}}\right]_{\mathcal{K}}$$

$$\left[\underline{W}_\varepsilon^{n,k}\right]_j = \frac{\widehat{\underline{r}}_j - \gamma\, M_{jj}\,[\underline{U}_\varepsilon^{n,k}]_j}{\tau_n\, A_{jj}^{n-1}}$$

Uzawa algorithm

Uzawa-Multigrid algorithm Gräser, Kornhuber (2005), derived from the formulation of Blowey, Elliott (1991, 1992),
Outer Uzawa-type iterations constrained minimisation, two sub-steps

- $\gamma\,(\underline{V} - \underline{U}_\varepsilon^{n,k})^T\,B\,\underline{U}_\varepsilon^{n,k} \geq (\underline{V} - \underline{U}_\varepsilon^{n,k})^T\,\underline{s} + (\underline{V} - \underline{U}_\varepsilon^{n,k})^T\,M\,\underline{W}_\varepsilon^{n,k-1} \qquad \forall\,\underline{V} \in \mathcal{K}^{\mathcal{J}}$
- $\underline{W}_\varepsilon^{n,k} = \underline{W}_\varepsilon^{n,k-1} + S^{-1}\left(-\gamma\,M\,\underline{U}_\varepsilon^{n,k} - \tau_n\,A^{n-1}\,\underline{W}_\varepsilon^{n,k-1} + \underline{r}\right)$

S^{-1} - preconditioner

Uzawa algorithm

Preconditioner

If we know the exact coincidence/contact set

$$\widehat{J}(\underline{U}^n_\varepsilon) = \left\{ j \in J : \left| [\underline{U}^n_\varepsilon]_j \right| = 1 \right\},$$

the problem becomes linear

$$\begin{pmatrix} \gamma\, \widehat{B}(\underline{U}^n_\varepsilon) & -\widehat{M}(\underline{U}^n_\varepsilon) \\ \gamma\, M & \tau_n\, A^{n-1} \end{pmatrix} \begin{pmatrix} \underline{U}^n_\varepsilon \\ \underline{W}^n_\varepsilon \end{pmatrix} = \begin{pmatrix} \widehat{s}(\underline{U}^n_\varepsilon) \\ \underline{r} \end{pmatrix}.$$

with

$$\widehat{B}_{ij} = \begin{cases} \delta_{ij} & i \in \widehat{J} \\ B_{ij} & \text{else} \end{cases},$$
$$\widehat{M}_{ij} = \begin{cases} 0 & i \in \widehat{J} \\ M_{ij} & \text{else} \end{cases}, \qquad j \in J,$$

and

$$\widehat{s}_i = \begin{cases} \gamma\, [\underline{U}^n_\varepsilon]_i & i \in \widehat{J} \\ s_i & \text{else} \end{cases}.$$

Uzawa algorithm

Optimal choice Schur complement

$$S(\underline{U}_\varepsilon^n) = M\widehat{B}(\underline{U}_\varepsilon^n)^{-1}\widehat{M}(\underline{U}_\varepsilon^n) + \tau_n\, A^{n-1}$$

Approximation $\underline{U}_\varepsilon^{n,k} \approx \underline{U}_\varepsilon^n$

$$S = S(\underline{U}_\varepsilon^{n,k}) = M\widehat{B}(\underline{U}_\varepsilon^{n,k})^{-1}\widehat{M}(\underline{U}_\varepsilon^{n,k}) + \tau_n\, A^{n-1}$$

Uzawa with the preconditioner $S(\underline{U}^k)$

$$\begin{aligned} \gamma\,(\underline{V} - \underline{U}_\varepsilon^{n,k})^T\, B\, \underline{U}_\varepsilon^{n,k} &\geq (\underline{V} - \underline{U}_\varepsilon^{n,k})^T\, \underline{s} + (\underline{V} - \underline{U}_\varepsilon^{n,k})^T\, M\, \underline{W}_\varepsilon^{n,k-1} \qquad \forall\, \underline{V} \in \mathcal{K}^{\mathcal{J}}, \\ \underline{W}_\varepsilon^{n,k} &= S(\underline{U}_\varepsilon^{n,k})^{-1}\left(-M\widehat{B}(\underline{U}_\varepsilon^{n,k})^{-1}\,\widehat{s}(\underline{U}_\varepsilon^{n,k}) + \underline{r}\right). \end{aligned}$$

Uzawa algorithm

Solution of the subproblems

- first step, elliptic variational inequality with double obstacle, we can use standard methods: projected Gauss-Seidel or Monotone multigrid; iterations can be stopped when we obtain convergence in the coincidence step - only few iterations.
  input $\underline{W}_{\varepsilon}^{n,k-1}$, output $\underline{U}_{\varepsilon}^{n,k}$

- second step is equivalent to the solution of linear symmetric saddle point problem

$$\begin{pmatrix} \gamma^2\,\widetilde{B} & -\gamma\,\widehat{M}(\underline{U}_{\varepsilon}^{n,k}) \\ -\gamma\,\widehat{M}(\underline{U}_{\varepsilon}^{n,k}) & -\tau_n\,A^{n-1} \end{pmatrix} \begin{pmatrix} \underline{\widetilde{U}}^{k} \\ \underline{W}_{\varepsilon}^{n,k} \end{pmatrix} = \begin{pmatrix} \gamma\,\widetilde{s} \\ -\widetilde{r} \end{pmatrix}$$

  standard W-cycle multigrid method for saddle point problems (Stokes equations, mixed FEM), canonical restriction and prolongation, block Gauss-Seidel smoother (1 smoothing step), alternative (Vanka type (1986)) smoother Schröberl, Zulehner (2003).
  input $\widehat{J}^k = \widehat{J}(\underline{U}_{\varepsilon}^{n,k})$, output $\underline{W}_{\varepsilon}^{n,k}$

Uzawa algorithm

Numerical implementation (more natural, but no proof of convergence)
$\Xi_\varepsilon(U_\varepsilon^{n-1}) \leftrightarrow \pi^h[b(U_\varepsilon^{n-1})]$, $\pi[b(U_\varepsilon^{n-1})] \equiv 0$ on J_{deg}
A^{n-1} - has zero rows due to the degeneracy of $b(\cdot)$

Degenerate set $j \in J_{deg} := \left\{ j \in J : \pi^h \left[b(U_\varepsilon^{n-1}) \right] \equiv 0 \text{ on } \mathrm{supp}(\chi_j) \right\}$
Solution
We use the fact $(J_{deg} \subset \widehat{J}^k)$ $\underline{U}_j^{n,k} = \underline{U}_j^{n-1}$ for all $j \in J_{deg}$ We obtain an equivalent saddle point problem with regular matrix A_{deg}^{-1}

$$\begin{pmatrix} \gamma^2 \widetilde{B} & -\gamma \widehat{M} \\ -\gamma \widehat{M} & -\tau_n A_{deg}^{n-1} \end{pmatrix} \begin{pmatrix} \underline{\widetilde{U}}^k \\ \underline{\widetilde{W}}^k \end{pmatrix} = \begin{pmatrix} \gamma \widetilde{s} \\ -\widetilde{r}_{deg} \end{pmatrix},$$

where $\underline{\widetilde{W}}_j = \underline{W}_j^{n-1}$ for $j \in J_{deg}$.

Uzawa algorithm

Complete algorithm

1. Initialization: Start with inital guess $\underline{U}_\varepsilon^{n,0} = \underline{U}_\varepsilon^{n-1}$, set $\widehat{J}^0 = \widehat{J}(\underline{U}_\varepsilon^{n,0})$ and compute $\underline{W}_\varepsilon^{n,0}$ by solving the linear saddle point problem with coincidence set $\widehat{J}^0$.

2. Uzawa iterations: for $k = 1, \dots$ do
   - 1st sub-step Compute the approximate coincidence set $\widehat{J}^k = \widehat{J}(\underline{U}_\varepsilon^{n,k})$, where $\underline{U}_\varepsilon^{n,k}$ is obtained from the elliptic variational inequality by PGS or MMG.
   - If $\widehat{J}^k = \widehat{J}^{k-1}$ go to step 3.
   - 2nd sub-step Solve a linear symmetric saddle point problem by the multigrid method with block Gauss–Seidel smoother to obtain $\underline{W}_\varepsilon^{n,k}$.
   - If $\max_{j \in J} | \left[\underline{W}_\varepsilon^{n,k}\right]_j - \left[\underline{W}_\varepsilon^{n,k-1}\right]_j | < tol$, with tol being the prescribed tolerance, go to step 3.

3. Uzawa iterations have converged: Compute $\underline{U}_\varepsilon^{n,k+1}$ up to the desired accuracy from the elliptic variational inequality from the 1st sub-step using $\underline{W}_\varepsilon^{n,k}$.

4. Set $\underline{U}_\varepsilon^n = \underline{U}_\varepsilon^{n,k+1}$, $\underline{W}_\varepsilon^n = \underline{W}_\varepsilon^{n,k}$.

Numerical experiments

FEM code Alberta; adaptive meshes:
if $|\underline{U}^n| < 1$ (i.e. in the interfacial region) set $h = h_{min} \approx \frac{1}{N_f}$ else $(|\underline{U}^n| = 1)$ set $h = h_{max} = \frac{1}{N_c}$.
Comparison of Uzawa and Gauss-Seidel methods $\gamma = \frac{1}{12\pi}$

N_f	τ	GS	Uzawa-MG	ratio
128	1e-6	14227m	3445m	4.13
64	4e-6	252m	146m	1.72
32	1.e-5	9m40s	11m20s	0.85

Table 1: Computation times for different values of h

γ	N_f	τ	GS	Uzawa-MG	ratio
$1/12\pi$	128	1e-6	14227m	3445m	4.13
$1/6\pi$	64	4e-6	853m	259m	3.29
$1/3\pi$	32	1.e-5	93m	30m	3.1

Table 2: Computational times for different values of γ

Multigrid algorithm - notation

Problem matrix on fine mesh

$$\mathcal{A} = \begin{pmatrix} B & -M \\ M & A \end{pmatrix}$$

Saddle point problem with variational inequality

$$\mathcal{A}\begin{pmatrix} \underline{U} \\ \underline{W} \end{pmatrix} \geq \begin{pmatrix} \underline{r} \\ \underline{s} \end{pmatrix} \qquad \underline{U} \in \mathcal{K}^{\mathcal{J}}$$

Intergrid transfer operators (canonical restriction and prolongation) I_f^c, I_c^f

Coarse matrix $\mathcal{A}_c$

$$\mathcal{A}_c = \begin{pmatrix} I_f^c\, B\, I_c^f & -I_f^c\, M\, I_c^f \\ I_f^c\, M\, I_c^f & I_f^c\, A\, I_c^f \end{pmatrix}$$

Multigrid algorithm

Two-grid scheme for the solution of

$$\mathcal{A}\begin{pmatrix} \underline{U} \\ \underline{W} \end{pmatrix} \geq \begin{pmatrix} \underline{r} \\ \underline{s} \end{pmatrix} \qquad \underline{U} \in \mathcal{K}^{\mathcal{J}}$$

- **pre smoothing**
  m iteration of projected Gauss-Seidel $(\underline{U}^0, \underline{W}^0) \to (\underline{U}^m, \underline{W}^m)$

- **coarse grid correction** solve the coarse problem exactly

  1. compute residual $(\underline{Q}^u, \underline{Q}^w) = (\underline{r}, \underline{s}) - \mathcal{A}(\underline{U}^m, \underline{W}^m)$
  2. $$\mathcal{A}_c\begin{pmatrix} \underline{V}^u \\ \underline{V}^w \end{pmatrix} \geq \begin{pmatrix} I_f^c \underline{Q}^u \\ I_f^c \underline{Q}^w \end{pmatrix} \qquad \underline{V}^u \in \mathcal{K}_*^{\mathcal{J}_c}$$
  3. update solution $(\underline{U}^{m+1}, \underline{W}^{m+1}) = (\underline{U}^m + I_c^f \underline{V}^u, \underline{W}^m + I_c^f \underline{V}^w)$

- **post smoothing**
  m iteration of projected Gauss-Seidel $(\underline{U}^{m+1}, \underline{W}^{m+1}) \to (\underline{U}^{2m+1}, \underline{W}^{2m+1})$

Coarse grid correction

We require

$$|\underline{U}^{m+1} + I_c^f \underline{V}^u| \leq 1$$

New obstacle for $\underline{V}^u$

$$-1 - \underline{U}^{m+1} \leq I_c^f \underline{V}^u \leq 1 - \underline{U}^{m+1}$$

associated with the fine mesh, but to compute $\underline{V}^u$ on the coarse grid we need a "coarse obstacle".

Solution Mandel (1984) look for $\underline{V}^u \in K_*^{\mathcal{J}_c}$ where
$\mathcal{K}_*^{\mathcal{J}_c} = \left\{\underline{V} \in \mathbb{R}^{\mathcal{J}_c}; Q_f^c(-1 - \underline{U}^{m+1}) \leq \underline{V} \leq R_f^c(-1 - \underline{U}^{m+1})\right\}$ with upper/lower obstacle restriction operators defined as

$$\begin{aligned} \left[Q_f^c v\right](p) &= \max\left\{v(q);\, q \in \mathcal{N}^f \cap \operatorname{int}\operatorname{supp}\chi^p,\, \chi^p \in V_h^c\right\}, \\ \left[R_f^c v\right](p) &= \min\left\{v(q);\, q \in \mathcal{N}^f \cap \operatorname{int}\operatorname{supp}\chi^p,\, \chi^p \in V_h^c\right\}, \end{aligned}$$

with $\quad p \in \mathcal{N}^{k-1},\, v \in V_h^f$.
Kornhuber (1994) slightly better obstacle restriction (suitable linear combination instead of min/max).

Coarse grid correction - mltiple grids

Restrictions for numerical convergence grid on the lowest has to be fine enough; number of grid levels depends on γ and h_{min}, we need:

- small γ for good approximation of the sharp interface problem
- small h_{min} (depending on γ) for good approximation of the continuous phase-field model

Feasible parameter combnations in 3D

- $\gamma = \frac{1}{12\pi}$, $N_f = \frac{1}{128}$, 6 mesh points in the interface, 2-level method
- $\gamma = \frac{1}{9\pi}$, $N_f = \frac{1}{128}$, 8 mesh points in the interface, 3-level method

Coarse grid solver inexact solution with projected GS, 30 iteration are enough for the 3-level method.

Numerical experiments

Meshes on different levels

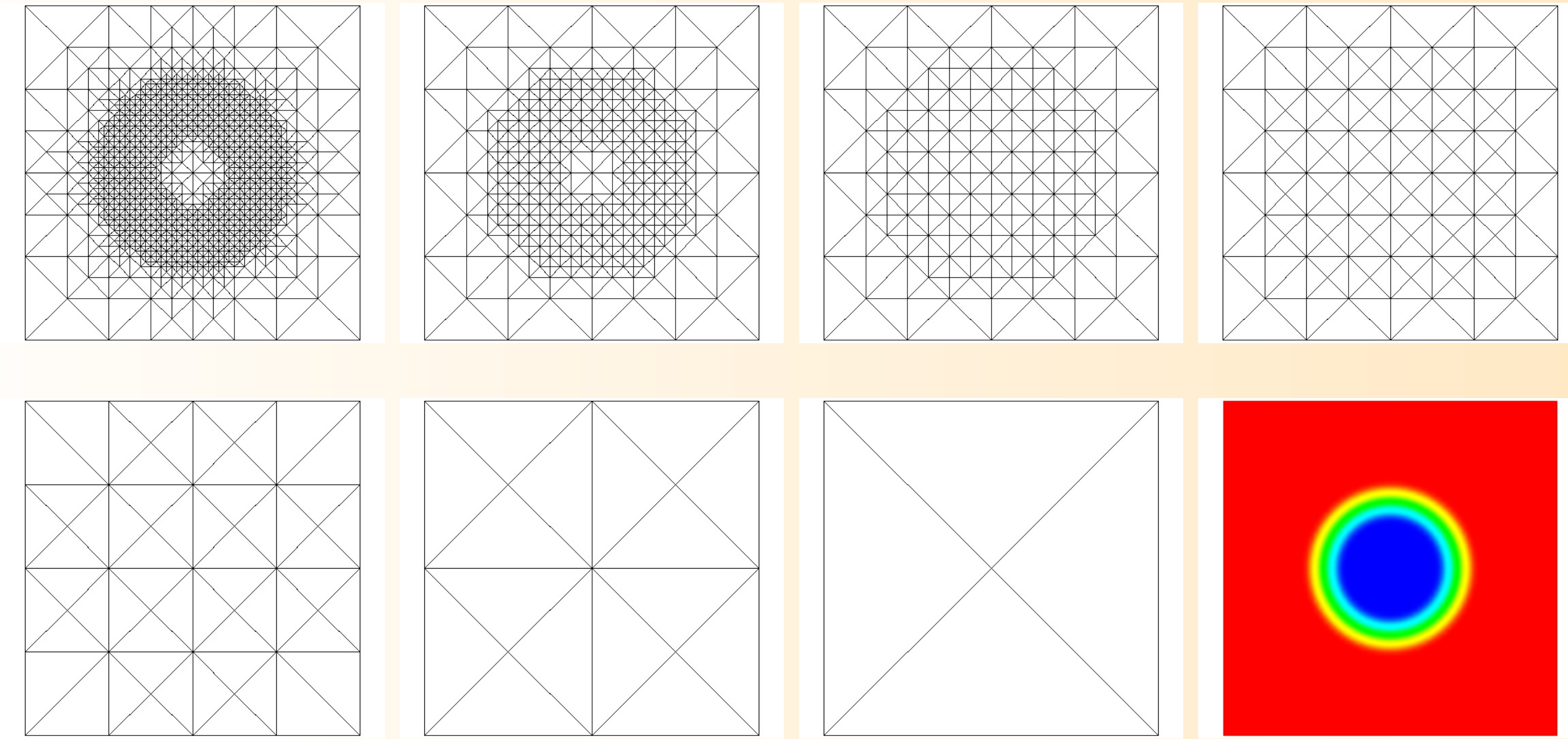

Comparison of the Multigrid and Uzawa methods

3D computation with about 900000 degrees of freedom, $\gamma = \frac{1}{9\pi}$

method	total iteration	CPU time
MG	2063	2200m
Uzawa-MG	4760	3390m

Table 3: 3-level MG vs. Uzawa (8-level); W-cycle, 1 smoothing step

Multigrid computations are about 1.5 times faster with $2\times$ less iterations.

Numerical experiments

$\gamma = \frac{1}{12\pi}$, $T = 0.06$, $\tau = 10^{-6}$, $N_f = 128$, $N_c = 2$

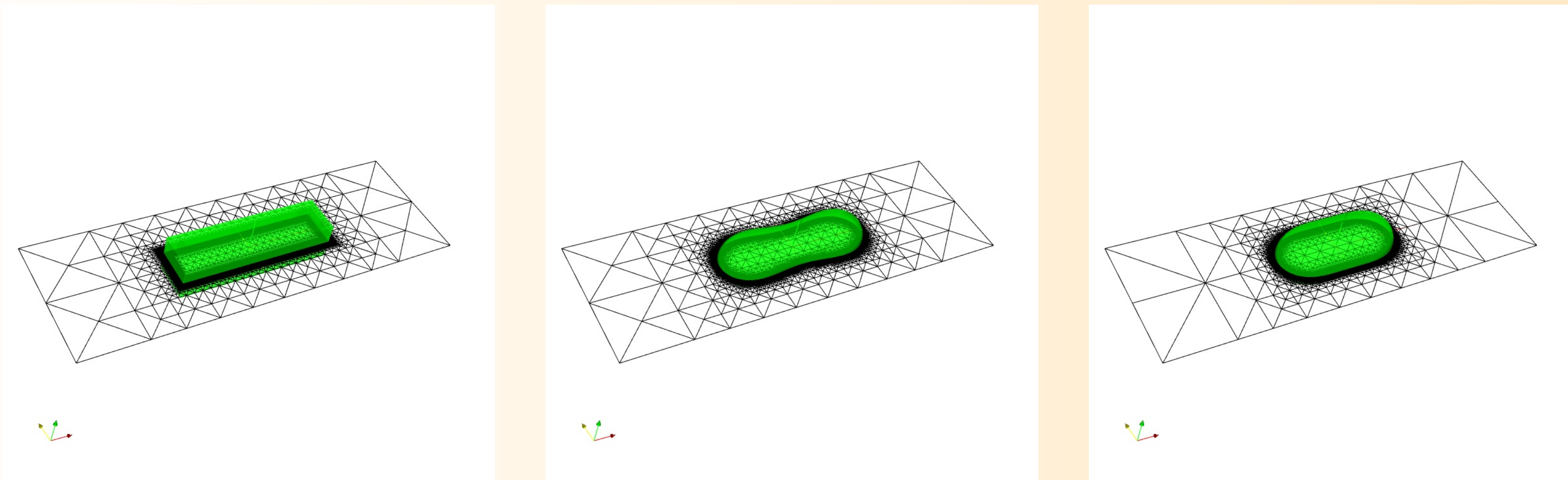

Figure 1: $(\alpha = 0)$ Zero level sets for $U_\varepsilon(x,t)$, with cut through the mesh at $x_3 = 0$ at times $t = 0, 0.001, 0.005$.

Numerical experiments

$\gamma = \frac{1}{12\pi}$, $T = 0.06$, $\tau = 10^{-6}$, $N_f = 128$, $N_c = 2$

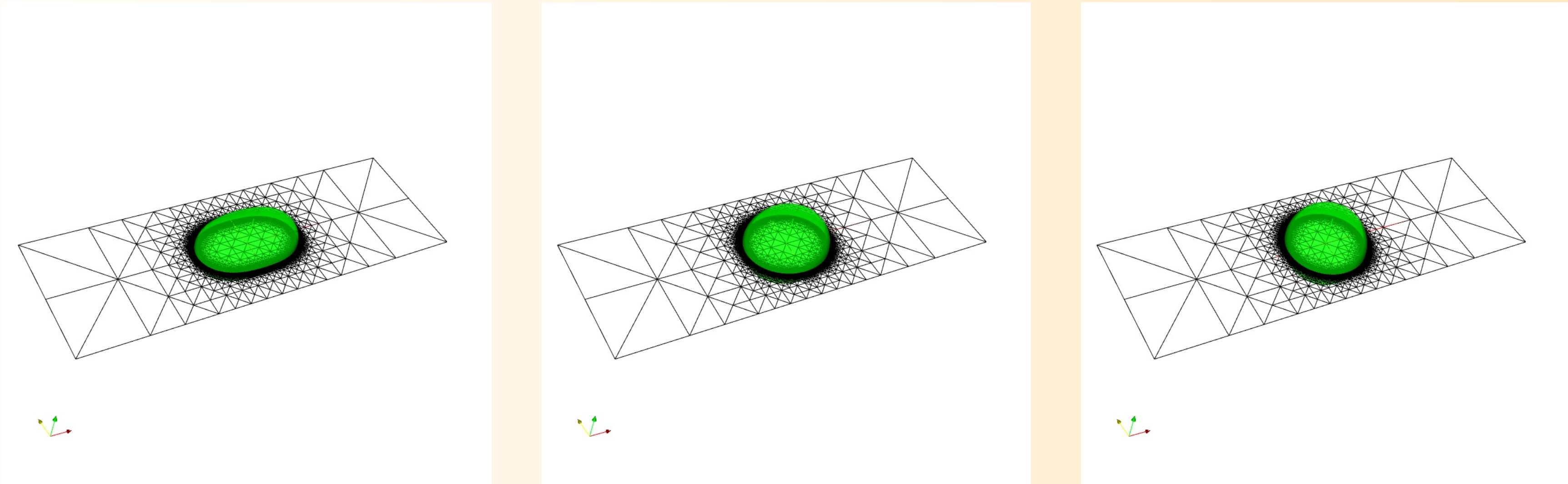

Figure 2: $(\alpha = 0)$ Zero level sets for $U_\varepsilon(x,t)$, with cut through the mesh at $x_3 = 0$ at times $t = 0.01, 0.015, T = 0.06$.

Numerical experiments

$\gamma = \frac{1}{12\pi}$, $T = 0.08$, $\tau = 5 \times 10^{-6}$, $N_f = 48$, $N_c = 2$

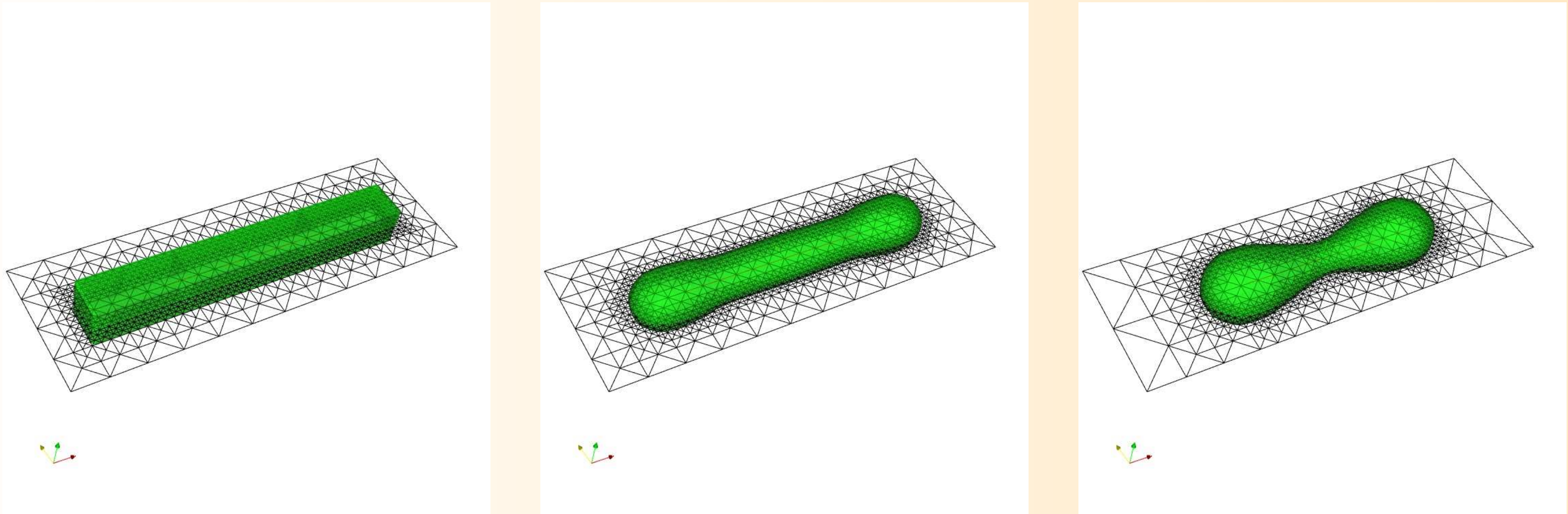

Figure 3: ($\alpha = 0$) Zero level sets for $U_\varepsilon(x,t)$, with cut through the mesh at $x_3 = 0$ at times $t = 0, 0.001, 0.005$.

Numerical experiments

$\gamma = \frac{1}{12\pi}$, $T = 0.08$, $\tau = 5 \times 10^{-6}$, $N_f = 48$, $N_c = 2$

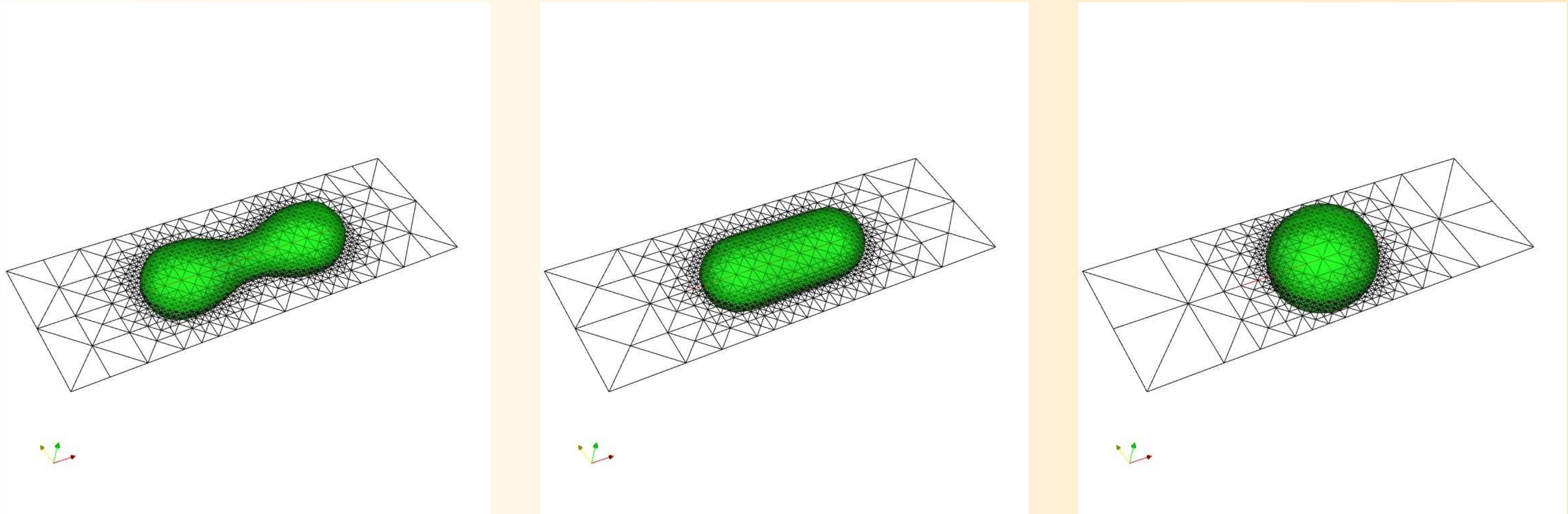

Figure 4: $(\alpha = 0)$ Zero level sets for $U_\varepsilon(x,t)$, with cut through the mesh at $x_3 = 0$ at times $t = 0.01, 0.015, T = 0.08$.

Numerical experiments

$\gamma = \frac{1}{12\pi}$, $T = 0.06$, $\tau = 1 \times 10^{-6}$, $N_f = 128$, $N_c = 2$

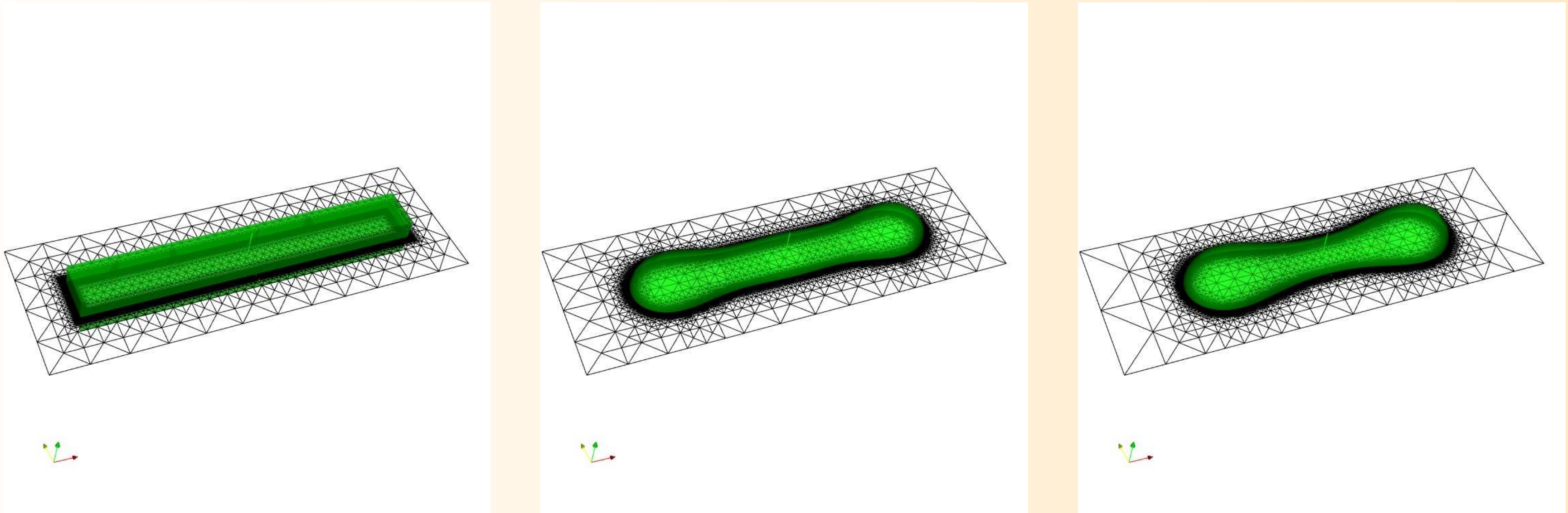

Figure 5: $(\alpha = 0)$ Zero level sets for $U_\varepsilon(x,t)$, with cut through the mesh at $x_3 = 0$ at times $t = 0, 0.0015, 0.003$.

Numerical experiments

$\gamma = \frac{1}{12\pi}$, $T = 0.06$, $\tau = 1 \times 10^{-6}$, $N_f = 128$, $N_c = 2$

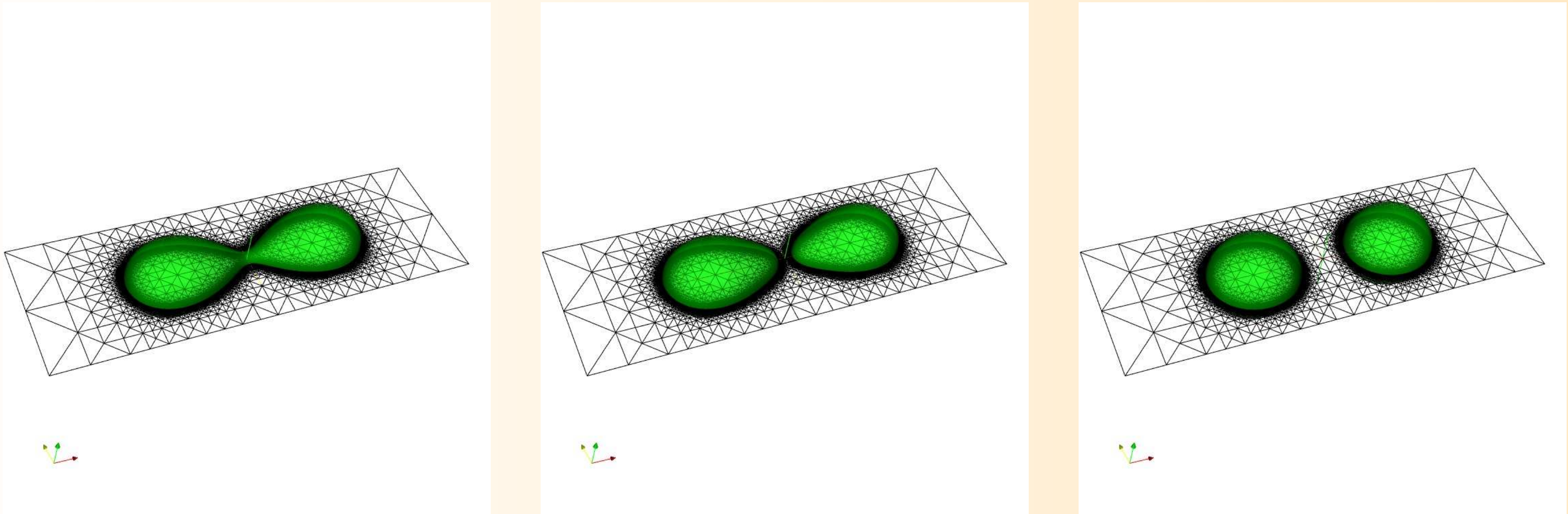

Figure 6: ($\alpha = 0$) Zero level sets for $U_\varepsilon(x,t)$, with cut through the mesh at $x_3 = 0$ at times $t = 0.00505, 0.0051, T = 0.06$.

Numerical experiments

$\gamma = \frac{1}{12\pi}$, $T = 0.001$,$\tau = 10^{-5}$, $N_f = 64$, $N_c = 2$

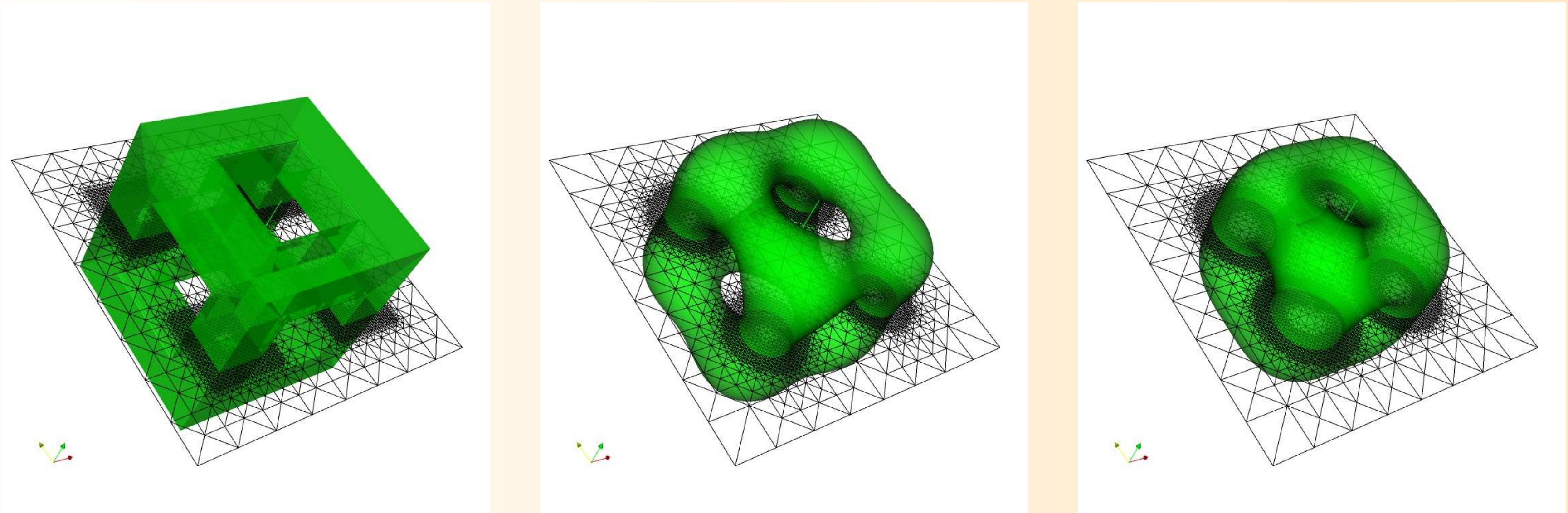

Figure 7: $(\alpha = 0)$ Zero level sets for $U_\varepsilon(x,t)$, with cut through the mesh at $x_3 = 0$ at times $t = 0, 1.5 \times 10^{-4}, 3.5 \times 10^{-4}$.

Numerical experiments

$\gamma = \frac{1}{12\pi}$, $T = 0.001$,$\tau = 10^{-5}$, $N_f = 64$, $N_c = 2$

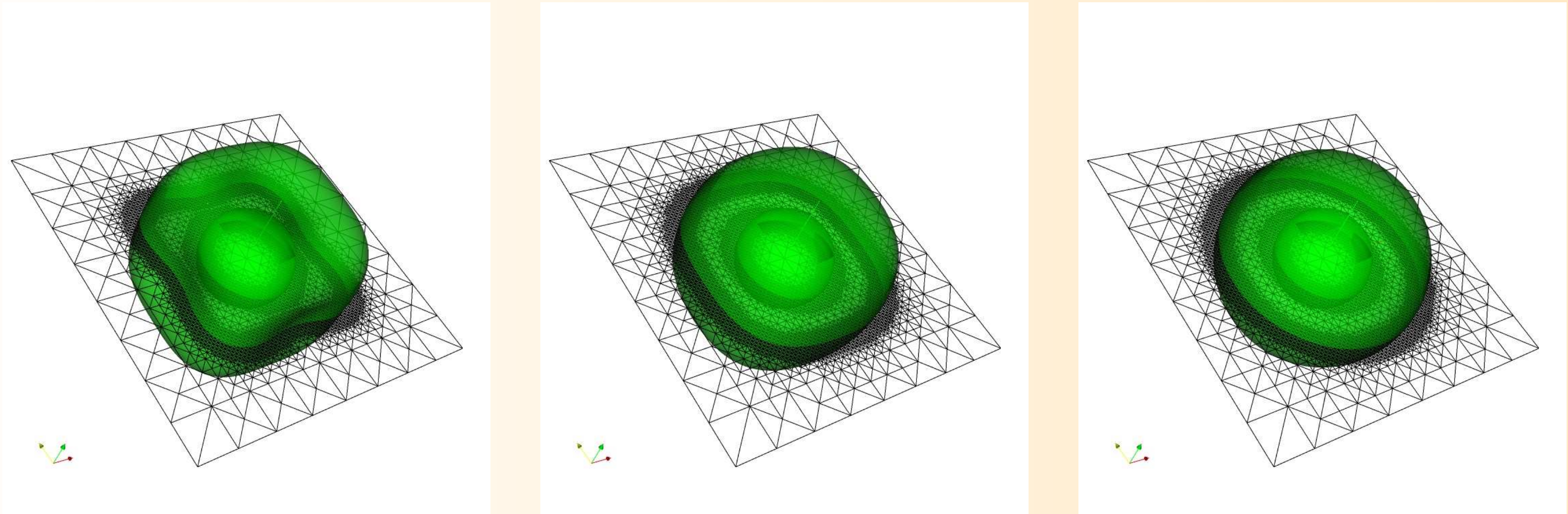

Figure 8: $(\alpha = 0)$ Zero level sets for $U_\varepsilon(x,t)$, with cut through the mesh at $x_3 = 0$ at times $t = 4\times 10^{-4}, 4.5\times 10^{-4}, 1\times 10^{-3}$.

Numerical experiments

$\alpha = 114$, $\gamma = \frac{1}{12\pi}$, $T = 5 \times 10^{-4}$, $\tau = 1 \times 10^{-7}$, $N_f = 128$, $N_c = 16$

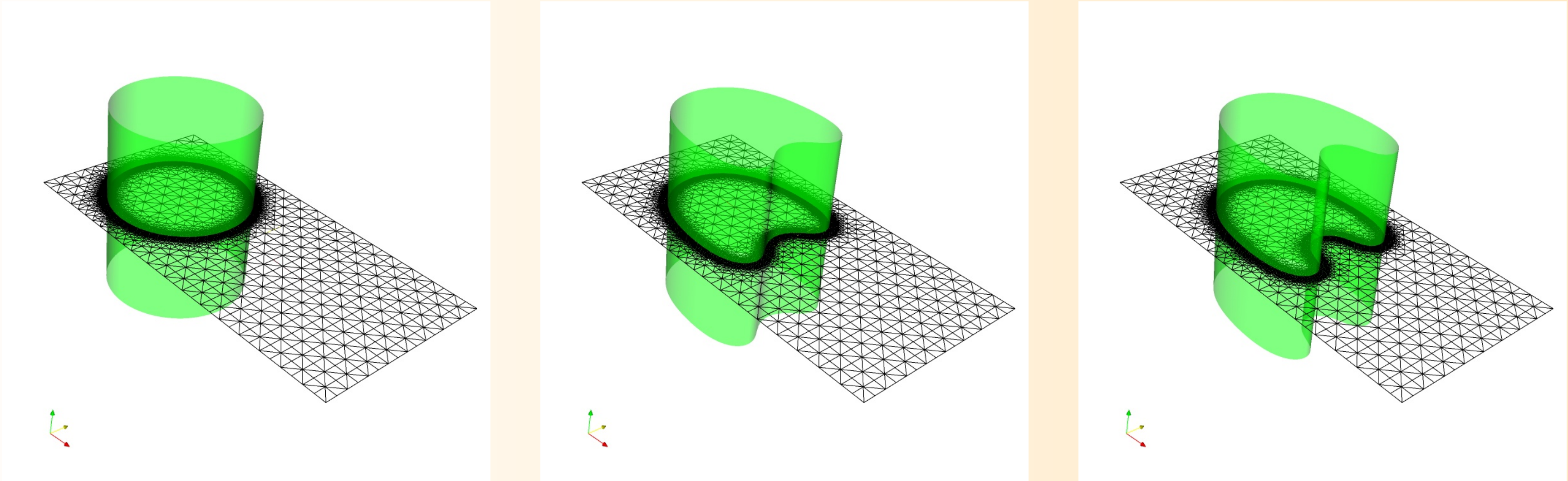

Figure 9: $(\alpha = 114\pi)$ Zero level sets for $U_\varepsilon(x,t)$, with cut through the mesh at $x_3 = 0$ at times $t = 0,\ 8 \times 10^{-5},\ 1.2 \times 10^{-5}$.

Numerical experiments

$\alpha = 114$, $\gamma = \frac{1}{12\pi}$, $T = 5 \times 10^{-4}$, $\tau = 1 \times 10^{-7}$, $N_f = 128$, $N_c = 16$

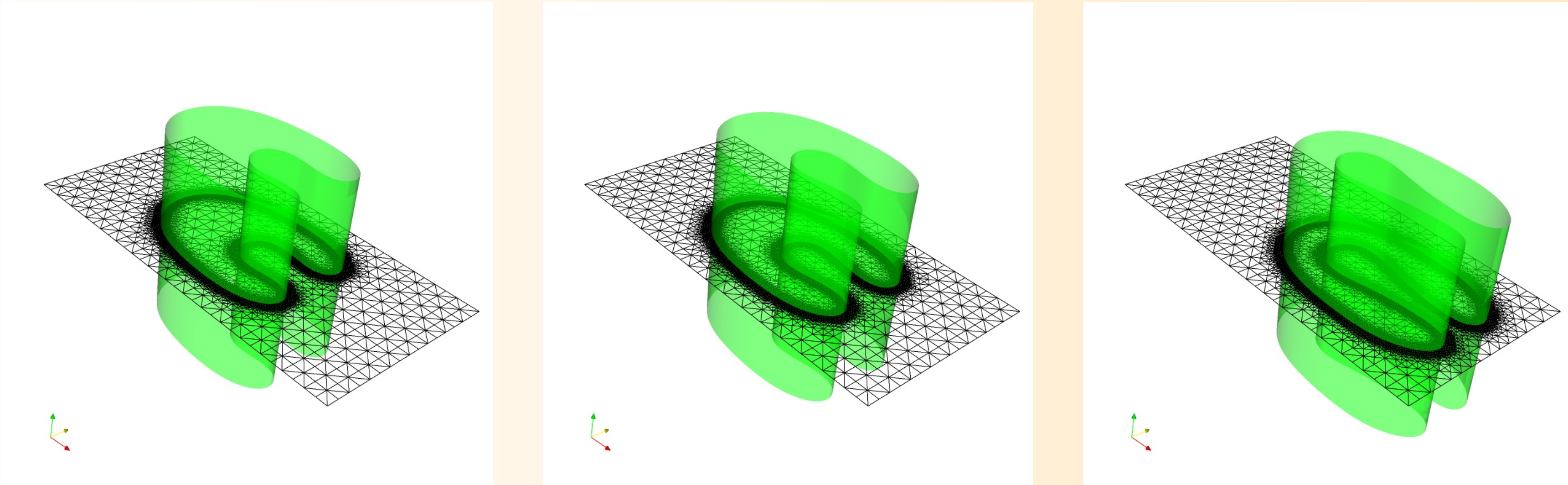

Figure 10: $(\alpha = 114\pi)$ Zero level sets for $U_\varepsilon(x,t)$, with cut through the mesh at $x_3 = 0$ at times $t = 2 \times 10^{-4}$, 2.4×10^{-4}, 3.6×10^{-4}.

Numerical experiments

$\alpha = 114$, $\gamma = \frac{1}{12\pi}$, $T = 5 \times 10^{-4}$, $\tau = 10^{-7}$, $N_f = 128$, $N_c = 16$

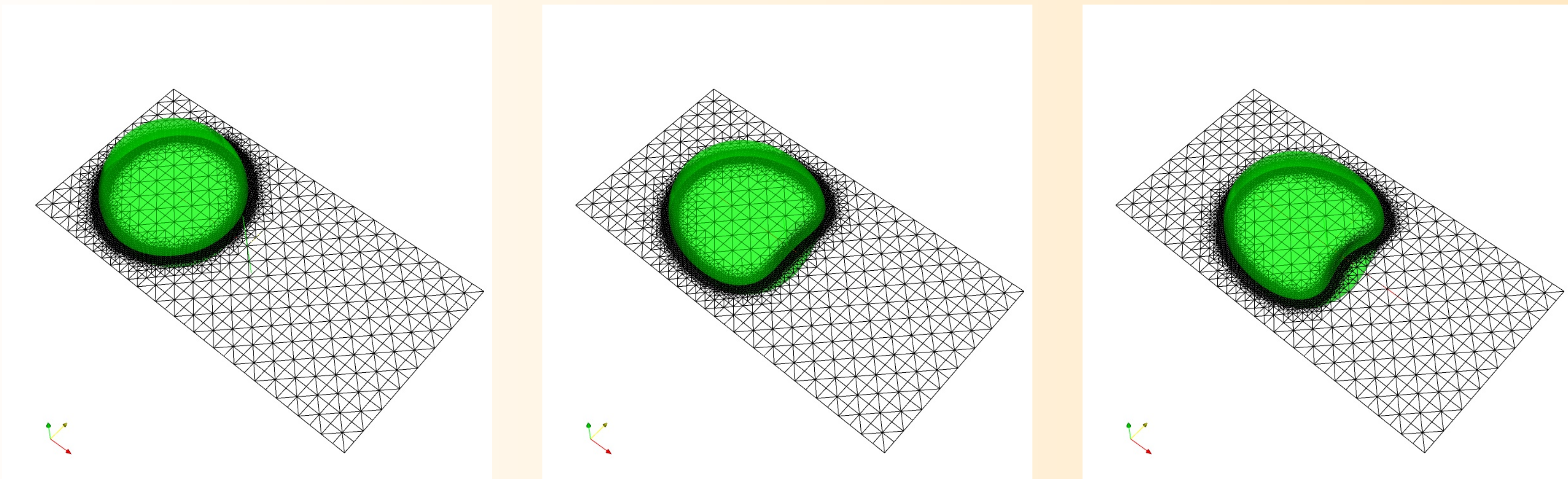

Figure 11: $(\alpha = 114\pi)$ Zero level sets for $U_\varepsilon(x,t)$, with cut through the mesh at $x_3 = 0$ at times $t = 0,\ 8 \times 10^{-5},\ 1.2 \times 10^{-5}$.

Numerical experiments

$\alpha = 114$, $\gamma = \frac{1}{12\pi}$, $T = 5 \times 10^{-4}$, $\tau = 10^{-7}$, $N_f = 128$, $N_c = 16$

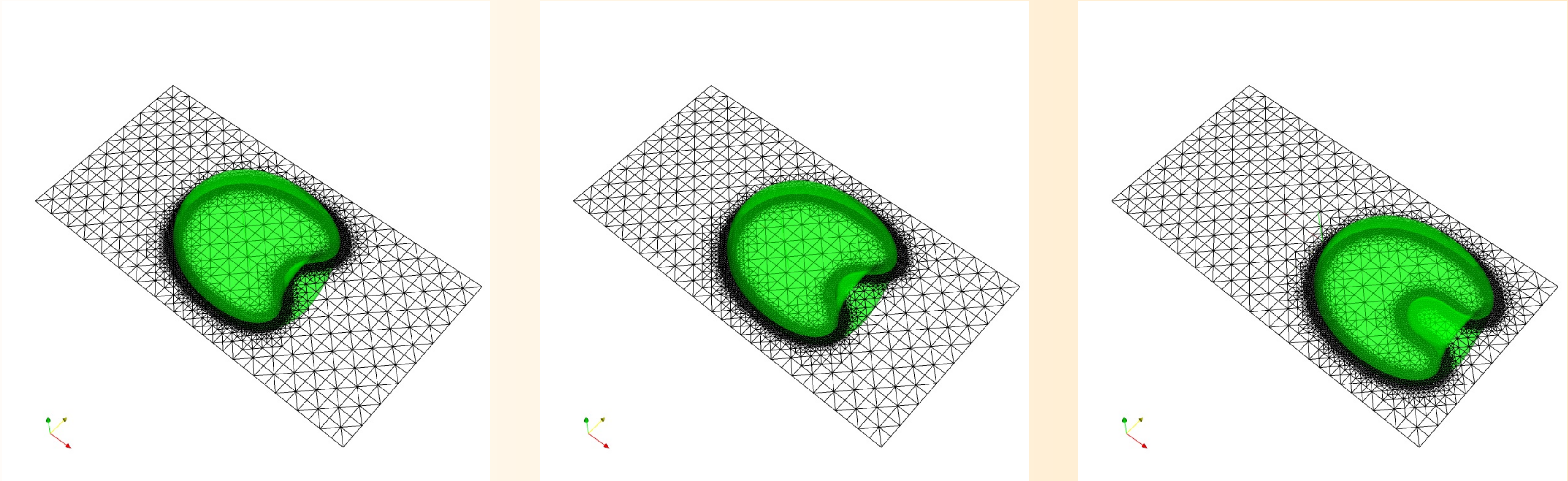

Figure 12: $(\alpha = 114\pi)$ Zero level sets for $U_\varepsilon(x,t)$, with cut through the mesh at $x_3 = 0$ at times $t = 2 \times 10^{-4}$, 2.4×10^{-4}, 3.6×10^{-4}.

Numerical experiments

$\alpha = 300$, $\gamma = \frac{1}{12\pi}$, $T = 1.25 \times 10^{-4}$, $\tau = 10^{-7}$, $N_f = 128$, $N_c = 16$

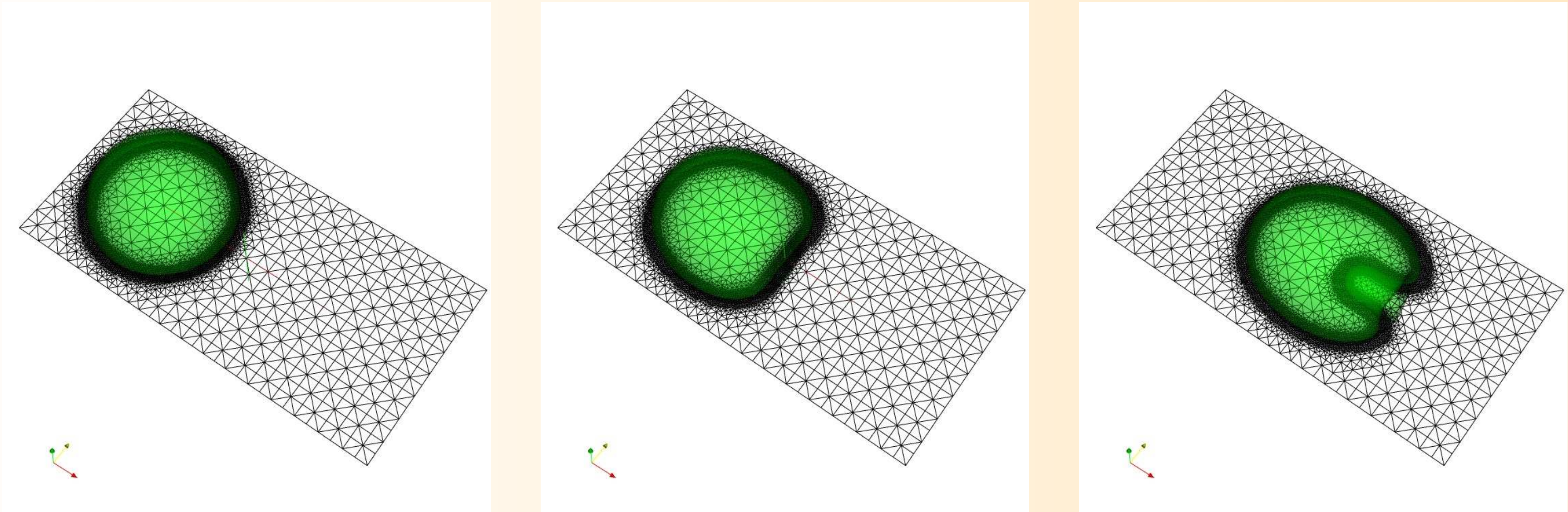

Figure 13: $(\alpha = 300\pi)$ Zero level sets for $U_\varepsilon(x,t)$, with cut through the mesh at $x_3 = 0$ at times $t = 0, 2.5 \times 10^{-5}, 7.5 \times 10^{-5}$.

Numerical experiments

$\alpha = 300$, $\gamma = \frac{1}{12\pi}$, $T = 1.25 \times 10^{-4}$, $\tau = 10^{-7}$, $N_f = 128$, $N_c = 16$

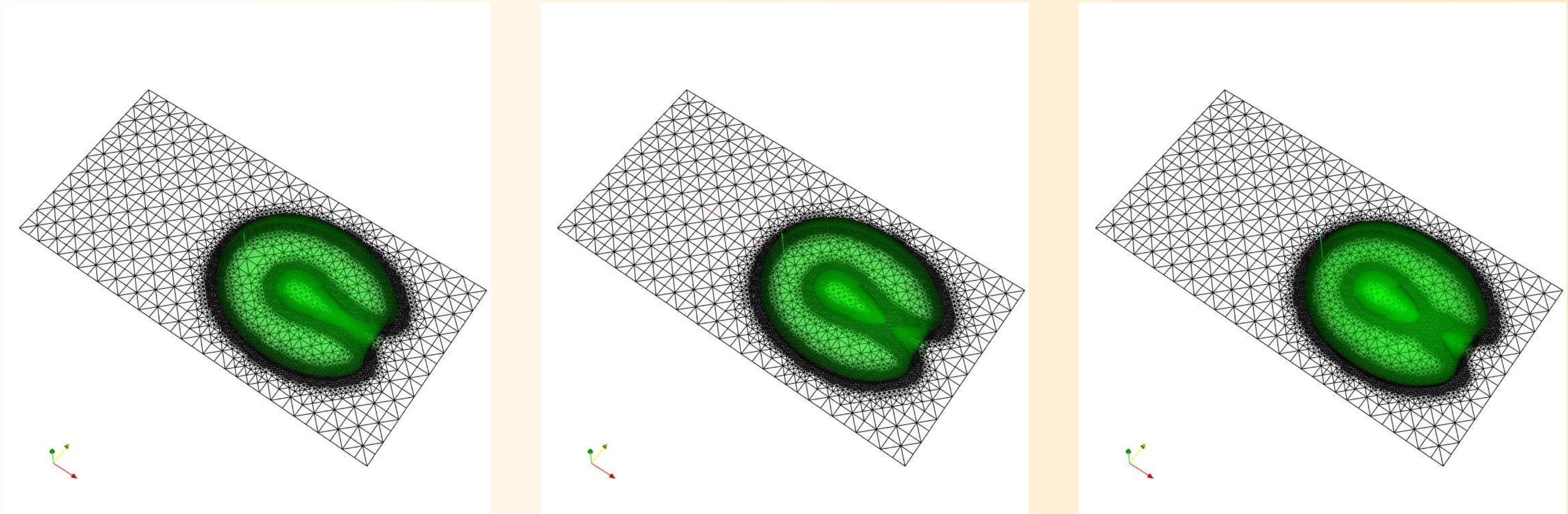

Figure 14: $(\alpha = 300\pi)$ Zero level sets for $U_\varepsilon(x,t)$, with cut through the mesh at $x_3 = 0$ at times $t = 1.15 \times 10^{-4}, 1.2 \times 10^{-4}, T = 1.25 \times 10^{-4}$.

Numerical experiments

$\alpha = 120$, $\gamma = \frac{1}{12\pi}$, $T = 2.7 \times 10^{-4}$, $\tau = 10^{-7}$, $N_f = 128$, $N_c = 16$

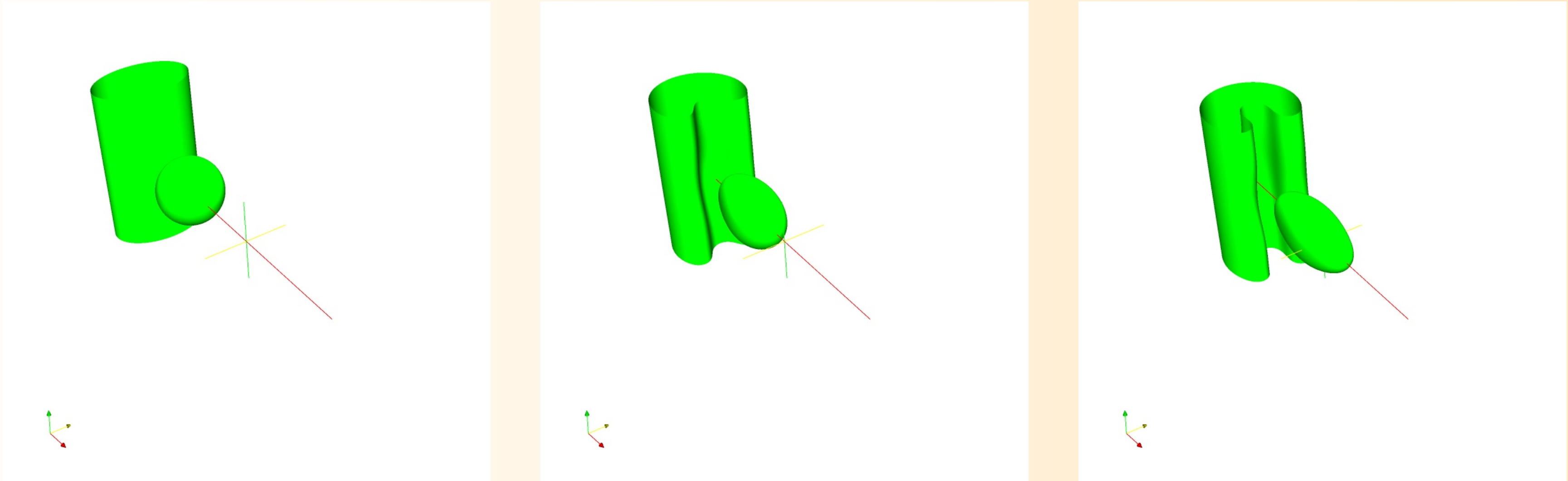

Figure 15: $(\alpha = 120\pi)$ Zero level sets for $U_\varepsilon(x,t)$ at times $t = 0, 7 \times 10^{-5}, 1.3 \times 10^{-4}$.

Numerical experiments

$\alpha = 120$, $\gamma = \frac{1}{12\pi}$, $T = 2.7 \times 10^{-4}$, $\tau = 10^{-7}$, $N_f = 128$, $N_c = 16$

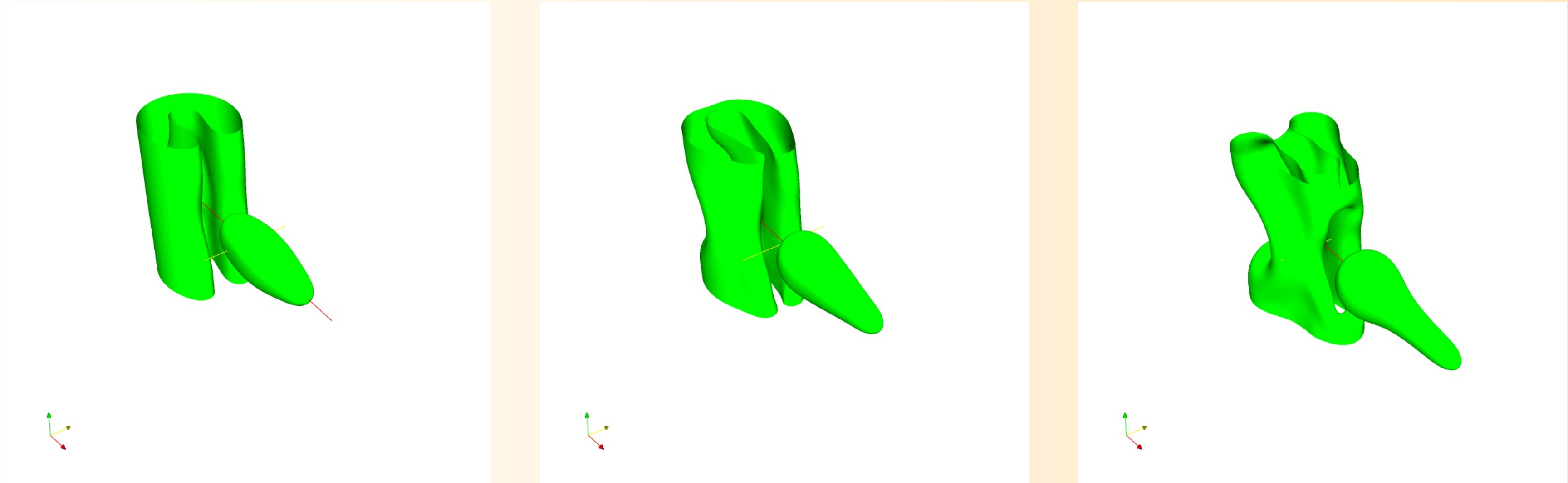

Figure 16: $(\alpha = 120\pi)$ Zero level sets for $U_\varepsilon(x,t)$ at times $t = 1.9 \times 10^{-4}, 2.3 \times 10^{-4}, T = 2.7 \times 10^{-4}$.

Final remarks

- fast coarse solver needed for efficiency
- limited flexibility with respect to γ
- robust except above remarks
- $\approx 2\times$ less iterations than Uzawa
- theory?